

Search for $b \rightarrow u$ transitions in $B^- \rightarrow [K^+\pi^-\pi^0]_D K^-$

The BABAR Collaboration

October 15, 2006

Abstract

We search for decays of a B meson into a neutral D meson and a kaon, with the D meson decaying into $K^+\pi^-\pi^0$. This final state can be reached through the $b \rightarrow c$ transition $B^- \rightarrow D^0 K^-$ followed by the doubly Cabibbo-suppressed $D^0 \rightarrow K^+\pi^-\pi^0$, or the $b \rightarrow u$ transition $B^- \rightarrow \bar{D}^0 K^-$ followed by the Cabibbo-favored $\bar{D}^0 \rightarrow K^+\pi^-\pi^0$. The interference of these two amplitudes is sensitive to the angle γ of the unitarity triangle. We present preliminary results based on 226×10^6 $e^+e^- \rightarrow \Upsilon(4S) \rightarrow B\bar{B}$ events collected with the BABAR detector at SLAC. We find no significant evidence for these decays and we set a limit $R_{ADS} \equiv \frac{\Gamma([K^+\pi^-\pi^0]_D K^-) + \Gamma([K^-\pi^+\pi^0]_D K^+)}{\Gamma([K^+\pi^-\pi^0]_D K^+) + \Gamma([K^-\pi^+\pi^0]_D K^-)} < 0.039$ at 95% confidence level, which we translate with a Bayesian approach into $r_B \equiv |A(B^- \rightarrow \bar{D}^0 K^-)/A(B^- \rightarrow D^0 K^-)| < 0.185$ at 95% confidence level.

Submitted to the 33rd International Conference on High-Energy Physics, ICHEP 06,
26 July—2 August 2006, Moscow, Russia.

Stanford Linear Accelerator Center, Stanford University, Stanford, CA 94309

Work supported in part by the US Department of Energy contract DE-AC02-76SF00515

The BABAR Collaboration,

B. Aubert, R. Barate, M. Bona, D. Boutigny, F. Couderc, Y. Karyotakis, J. P. Lees, V. Poireau,
V. Tisserand, A. Zghiche

*Laboratoire de Physique des Particules, IN2P3/CNRS et Université de Savoie, F-74941 Annecy-Le-Vieux,
France*

E. Grauges

Universitat de Barcelona, Facultat de Física, Departament ECM, E-08028 Barcelona, Spain

A. Palano

Università di Bari, Dipartimento di Fisica and INFN, I-70126 Bari, Italy

J. C. Chen, N. D. Qi, G. Rong, P. Wang, Y. S. Zhu

Institute of High Energy Physics, Beijing 100039, China

G. Eigen, I. Ofte, B. Stugu

University of Bergen, Institute of Physics, N-5007 Bergen, Norway

G. S. Abrams, M. Battaglia, D. N. Brown, J. Button-Shafer, R. N. Cahn, E. Charles, M. S. Gill,
Y. Groyzman, R. G. Jacobsen, J. A. Kadyk, L. T. Kerth, Yu. G. Kolomensky, G. Kukartsev, G. Lynch,
L. M. Mir, T. J. Orimoto, M. Pripstein, N. A. Roe, M. T. Ronan, W. A. Wenzel

Lawrence Berkeley National Laboratory and University of California, Berkeley, California 94720, USA

P. del Amo Sanchez, M. Barrett, K. E. Ford, A. J. Hart, T. J. Harrison, C. M. Hawkes, S. E. Morgan,
A. T. Watson

University of Birmingham, Birmingham, B15 2TT, United Kingdom

T. Held, H. Koch, B. Lewandowski, M. Pelizaeus, K. Peters, T. Schroeder, M. Steinke
Ruhr Universität Bochum, Institut für Experimentalphysik 1, D-44780 Bochum, Germany

J. T. Boyd, J. P. Burke, W. N. Cottingham, D. Walker

University of Bristol, Bristol BS8 1TL, United Kingdom

D. J. Asgeirsson, T. Cuhadar-Donszelmann, B. G. Fulsom, C. Hearty, N. S. Knecht, T. S. Mattison,
J. A. McKenna

University of British Columbia, Vancouver, British Columbia, Canada V6T 1Z1

A. Khan, P. Kyberd, M. Saleem, D. J. Sherwood, L. Teodorescu

Brunel University, Uxbridge, Middlesex UB8 3PH, United Kingdom

V. E. Blinov, A. D. Bukin, V. P. Druzhinin, V. B. Golubev, A. P. Onuchin, S. I. Serednyakov,
Yu. I. Skovpen, E. P. Solodov, K. Yu Todyshev

Budker Institute of Nuclear Physics, Novosibirsk 630090, Russia

D. S. Best, M. Bondioli, M. Bruinsma, M. Chao, S. Curry, I. Eschrich, D. Kirkby, A. J. Lankford, P. Lund,
M. Mandelkern, R. K. Mommsen, W. Roethel, D. P. Stoker

University of California at Irvine, Irvine, California 92697, USA

S. Abachi, C. Buchanan

University of California at Los Angeles, Los Angeles, California 90024, USA

S. D. Foulkes, J. W. Gary, O. Long, B. C. Shen, K. Wang, L. Zhang
University of California at Riverside, Riverside, California 92521, USA

H. K. Hadavand, E. J. Hill, H. P. Paar, S. Rahatlou, V. Sharma
University of California at San Diego, La Jolla, California 92093, USA

J. W. Berryhill, C. Campagnari, A. Cunha, B. Dahmes, T. M. Hong, D. Kovalskyi, J. D. Richman
University of California at Santa Barbara, Santa Barbara, California 93106, USA

T. W. Beck, A. M. Eisner, C. J. Flacco, C. A. Heusch, J. Kroseberg, W. S. Lockman, G. Nesom, T. Schalk,
B. A. Schumm, A. Seiden, P. Spradlin, D. C. Williams, M. G. Wilson
University of California at Santa Cruz, Institute for Particle Physics, Santa Cruz, California 95064, USA

J. Albert, E. Chen, A. Dvoretzkii, F. Fang, D. G. Hitlin, I. Narsky, T. Piatenko, F. C. Porter, A. Ryd,
A. Samuel
California Institute of Technology, Pasadena, California 91125, USA

G. Mancinelli, B. T. Meadows, K. Mishra, M. D. Sokoloff
University of Cincinnati, Cincinnati, Ohio 45221, USA

F. Blanc, P. C. Bloom, S. Chen, W. T. Ford, J. F. Hirschauer, A. Kreisel, M. Nagel, U. Nauenberg,
A. Olivas, W. O. Ruddick, J. G. Smith, K. A. Ulmer, S. R. Wagner, J. Zhang
University of Colorado, Boulder, Colorado 80309, USA

A. Chen, E. A. Eckhart, A. Soffer, W. H. Toki, R. J. Wilson, F. Winklmeier, Q. Zeng
Colorado State University, Fort Collins, Colorado 80523, USA

D. D. Altenburg, E. Feltresi, A. Hauke, H. Jasper, J. Merkel, A. Petzold, B. Spaan
Universität Dortmund, Institut für Physik, D-44221 Dortmund, Germany

T. Brandt, V. Klose, H. M. Lacker, W. F. Mader, R. Nogowski, J. Schubert, K. R. Schubert, R. Schwierz,
J. E. Sundermann, A. Volk
Technische Universität Dresden, Institut für Kern- und Teilchenphysik, D-01062 Dresden, Germany

D. Bernard, G. R. Bonneaud, E. Latour, Ch. Thiebaux, M. Verderi
Laboratoire Leprince-Ringuet, CNRS/IN2P3, Ecole Polytechnique, F-91128 Palaiseau, France

P. J. Clark, W. Gradl, F. Muheim, S. Playfer, A. I. Robertson, Y. Xie
University of Edinburgh, Edinburgh EH9 3JZ, United Kingdom

M. Andreotti, D. Bettoni, C. Bozzi, R. Calabrese, G. Cibinetto, E. Luppi, M. Negrini, A. Petrella,
L. Piemontese, E. Prencipe
Università di Ferrara, Dipartimento di Fisica and INFN, I-44100 Ferrara, Italy

F. Anulli, R. Baldini-Ferrolì, A. Calcaterra, R. de Sangro, G. Finocchiaro, S. Pacetti, P. Patteri,
I. M. Peruzzi,¹ M. Piccolo, M. Rama, A. Zallo
Laboratori Nazionali di Frascati dell'INFN, I-00044 Frascati, Italy

¹Also with Università di Perugia, Dipartimento di Fisica, Perugia, Italy

A. Buzzo, R. Capra, R. Contri, M. Lo Vetere, M. M. Macri, M. R. Monge, S. Passaggio, C. Patrignani,
E. Robutti, A. Santroni, S. Tosi

Università di Genova, Dipartimento di Fisica and INFN, I-16146 Genova, Italy

G. Brandenburg, K. S. Chaisanguanthum, M. Morii, J. Wu

Harvard University, Cambridge, Massachusetts 02138, USA

R. S. Dubitzky, J. Marks, S. Schenk, U. Uwer

Universität Heidelberg, Physikalisches Institut, Philosophenweg 12, D-69120 Heidelberg, Germany

D. J. Bard, W. Bhimji, D. A. Bowerman, P. D. Dauncey, U. Egede, R. L. Flack, J. A. Nash,
M. B. Nikolich, W. Panduro Vazquez

Imperial College London, London, SW7 2AZ, United Kingdom

P. K. Behera, X. Chai, M. J. Charles, U. Mallik, N. T. Meyer, V. Ziegler

University of Iowa, Iowa City, Iowa 52242, USA

J. Cochran, H. B. Crawley, L. Dong, V. Eyges, W. T. Meyer, S. Prell, E. I. Rosenberg, A. E. Rubin

Iowa State University, Ames, Iowa 50011-3160, USA

A. V. Gritsan

Johns Hopkins University, Baltimore, Maryland 21218, USA

A. G. Denig, M. Fritsch, G. Schott

Universität Karlsruhe, Institut für Experimentelle Kernphysik, D-76021 Karlsruhe, Germany

N. Arnaud, M. Davier, G. Grosdidier, A. Höcker, F. Le Diberder, V. Lepeltier, A. M. Lutz, A. Oyanguren,
S. Pruvot, S. Rodier, P. Roudeau, M. H. Schune, A. Stocchi, W. F. Wang, G. Wormser

*Laboratoire de l'Accélérateur Linéaire, IN2P3/CNRS et Université Paris-Sud 11, Centre Scientifique
d'Orsay, B.P. 34, F-91898 ORSAY Cedex, France*

C. H. Cheng, D. J. Lange, D. M. Wright

Lawrence Livermore National Laboratory, Livermore, California 94550, USA

C. A. Chavez, I. J. Forster, J. R. Fry, E. Gabathuler, R. Gamet, K. A. George, D. E. Hutchcroft,
D. J. Payne, K. C. Schofield, C. Touramanis

University of Liverpool, Liverpool L69 7ZE, United Kingdom

A. J. Bevan, F. Di Lodovico, W. Menges, R. Sacco

Queen Mary, University of London, E1 4NS, United Kingdom

G. Cowan, H. U. Flaecher, D. A. Hopkins, P. S. Jackson, T. R. McMahon, S. Ricciardi, F. Salvatore,
A. C. Wren

*University of London, Royal Holloway and Bedford New College, Egham, Surrey TW20 0EX, United
Kingdom*

D. N. Brown, C. L. Davis

University of Louisville, Louisville, Kentucky 40292, USA

J. Allison, N. R. Barlow, R. J. Barlow, Y. M. Chia, C. L. Edgar, G. D. Lafferty, M. T. Naisbit,
J. C. Williams, J. I. Yi

University of Manchester, Manchester M13 9PL, United Kingdom

C. Chen, W. D. Hulsbergen, A. Jawahery, C. K. Lae, D. A. Roberts, G. Simi

University of Maryland, College Park, Maryland 20742, USA

G. Blaylock, C. Dallapiccola, S. S. Hertzbach, X. Li, T. B. Moore, S. Saremi, H. Staengle

University of Massachusetts, Amherst, Massachusetts 01003, USA

R. Cowan, G. Sciolla, S. J. Sekula, M. Spitznagel, F. Taylor, R. K. Yamamoto

*Massachusetts Institute of Technology, Laboratory for Nuclear Science, Cambridge, Massachusetts 02139,
USA*

H. Kim, S. E. McLachlin, P. M. Patel, S. H. Robertson

McGill University, Montréal, Québec, Canada H3A 2T8

A. Lazzaro, V. Lombardo, F. Palombo

Università di Milano, Dipartimento di Fisica and INFN, I-20133 Milano, Italy

J. M. Bauer, L. Cremaldi, V. Eschenburg, R. Godang, R. Kroeger, D. A. Sanders, D. J. Summers,
H. W. Zhao

University of Mississippi, University, Mississippi 38677, USA

S. Brunet, D. Côté, M. Simard, P. Taras, F. B. Viaud

Université de Montréal, Physique des Particules, Montréal, Québec, Canada H3C 3J7

H. Nicholson

Mount Holyoke College, South Hadley, Massachusetts 01075, USA

N. Cavallo,² G. De Nardo, F. Fabozzi,³ C. Gatto, L. Lista, D. Monorchio, P. Paolucci, D. Piccolo,
C. Sciacca

Università di Napoli Federico II, Dipartimento di Scienze Fisiche and INFN, I-80126, Napoli, Italy

M. A. Baak, G. Raven, H. L. Snoek

*NIKHEF, National Institute for Nuclear Physics and High Energy Physics, NL-1009 DB Amsterdam, The
Netherlands*

C. P. Jessop, J. M. LoSecco

University of Notre Dame, Notre Dame, Indiana 46556, USA

T. Allmendinger, G. Benelli, L. A. Corwin, K. K. Gan, K. Honscheid, D. Hufnagel, P. D. Jackson,
H. Kagan, R. Kass, A. M. Rahimi, J. J. Regensburger, R. Ter-Antonyan, Q. K. Wong

Ohio State University, Columbus, Ohio 43210, USA

N. L. Blount, J. Brau, R. Frey, O. Igonkina, J. A. Kolb, M. Lu, R. Rahmat, N. B. Sinev, D. Strom,
J. Strube, E. Torrence

University of Oregon, Eugene, Oregon 97403, USA

²Also with Università della Basilicata, Potenza, Italy

³Also with Università della Basilicata, Potenza, Italy

A. Gaz, M. Margoni, M. Morandin, A. Pompili, M. Posocco, M. Rotondo, F. Simonetto, R. Stroili, C. Voci
Università di Padova, Dipartimento di Fisica and INFN, I-35131 Padova, Italy

M. Benayoun, H. Briand, J. Chauveau, P. David, L. Del Buono, Ch. de la Vaissière, O. Hamon,
B. L. Hartfiel, M. J. J. John, Ph. Leruste, J. Malcès, J. Ocariz, L. Roos, G. Therin
*Laboratoire de Physique Nucléaire et de Hautes Energies, IN2P3/CNRS, Université Pierre et Marie
Curie-Paris6, Université Denis Diderot-Paris7, F-75252 Paris, France*

L. Gladney, J. Panetta
University of Pennsylvania, Philadelphia, Pennsylvania 19104, USA

M. Biasini, R. Covarelli
Università di Perugia, Dipartimento di Fisica and INFN, I-06100 Perugia, Italy

C. Angelini, G. Batignani, S. Bettarini, F. Bucci, G. Calderini, M. Carpinelli, R. Cenci, F. Forti,
M. A. Giorgi, A. Lusiani, G. Marchiori, M. A. Mazur, M. Morganti, N. Neri, E. Paoloni, G. Rizzo,
J. J. Walsh
Università di Pisa, Dipartimento di Fisica, Scuola Normale Superiore and INFN, I-56127 Pisa, Italy

M. Haire, D. Judd, D. E. Wagoner
Prairie View A&M University, Prairie View, Texas 77446, USA

J. Biesiada, N. Danielson, P. Elmer, Y. P. Lau, C. Lu, J. Olsen, A. J. S. Smith, A. V. Telnov
Princeton University, Princeton, New Jersey 08544, USA

F. Bellini, G. Cavoto, A. D’Orazio, D. del Re, E. Di Marco, R. Faccini, F. Ferrarotto, F. Ferroni,
M. Gaspero, L. Li Gioi, M. A. Mazzoni, S. Morganti, G. Piredda, F. Polci, F. Safai Tehrani, C. Voena
Università di Roma La Sapienza, Dipartimento di Fisica and INFN, I-00185 Roma, Italy

M. Ebert, H. Schröder, R. Waldi
Universität Rostock, D-18051 Rostock, Germany

T. Adye, N. De Groot, B. Franek, E. O. Olaiya, F. F. Wilson
Rutherford Appleton Laboratory, Chilton, Didcot, Oxon, OX11 0QX, United Kingdom

R. Aleksan, S. Emery, A. Gaidot, S. F. Ganzhur, G. Hamel de Monchenault, W. Kozanecki, M. Legendre,
G. Vasseur, Ch. Yèche, M. Zito
DSM/Daphnia, CEA/Saclay, F-91191 Gif-sur-Yvette, France

X. R. Chen, H. Liu, W. Park, M. V. Purohit, J. R. Wilson
University of South Carolina, Columbia, South Carolina 29208, USA

M. T. Allen, D. Aston, R. Bartoldus, P. Bechtle, N. Berger, R. Claus, J. P. Coleman, M. R. Convery,
M. Cristinziani, J. C. Dingfelder, J. Dorfan, G. P. Dubois-Felsmann, D. Dujmic, W. Dunwoodie,
R. C. Field, T. Glanzman, S. J. Gowdy, M. T. Graham, P. Grenier,⁴ V. Halyo, C. Hast, T. Hryn’ova,
W. R. Innes, M. H. Kelsey, P. Kim, D. W. G. S. Leith, S. Li, S. Luitz, V. Luth, H. L. Lynch,
D. B. MacFarlane, H. Marsiske, R. Messner, D. R. Muller, C. P. O’Grady, V. E. Ozcan, A. Perazzo,
M. Perl, T. Pulliam, B. N. Ratcliff, A. Roodman, A. A. Salnikov, R. H. Schindler, J. Schwiening,
A. Snyder, J. Stelzer, D. Su, M. K. Sullivan, K. Suzuki, S. K. Swain, J. M. Thompson, J. Va’vra, N. van

⁴Also at Laboratoire de Physique Corpusculaire, Clermont-Ferrand, France

Bakel, M. Weaver, A. J. R. Weinstein, W. J. Wisniewski, M. Wittgen, D. H. Wright, A. K. Yarritu, K. Yi,
C. C. Young

Stanford Linear Accelerator Center, Stanford, California 94309, USA

P. R. Burchat, A. J. Edwards, S. A. Majewski, B. A. Petersen, C. Roat, L. Wilden

Stanford University, Stanford, California 94305-4060, USA

S. Ahmed, M. S. Alam, R. Bula, J. A. Ernst, V. Jain, B. Pan, M. A. Saeed, F. R. Wappler, S. B. Zain

State University of New York, Albany, New York 12222, USA

W. Bugg, M. Krishnamurthy, S. M. Spanier

University of Tennessee, Knoxville, Tennessee 37996, USA

R. Eckmann, J. L. Ritchie, A. Satpathy, C. J. Schilling, R. F. Schwitters

University of Texas at Austin, Austin, Texas 78712, USA

J. M. Izen, X. C. Lou, S. Ye

University of Texas at Dallas, Richardson, Texas 75083, USA

F. Bianchi, F. Gallo, D. Gamba

Università di Torino, Dipartimento di Fisica Sperimentale and INFN, I-10125 Torino, Italy

M. Bomben, L. Bosisio, C. Cartaro, F. Cossutti, G. Della Ricca, S. Dittongo, L. Lanceri, L. Vitale

Università di Trieste, Dipartimento di Fisica and INFN, I-34127 Trieste, Italy

V. Azzolini, N. Lopez-March, F. Martinez-Vidal

IFIC, Universitat de Valencia-CSIC, E-46071 Valencia, Spain

Sw. Banerjee, B. Bhuyan, C. M. Brown, D. Fortin, K. Hamano, R. Kowalewski, I. M. Nugent, J. M. Roney,
R. J. Sobie

University of Victoria, Victoria, British Columbia, Canada V8W 3P6

J. J. Back, P. F. Harrison, T. E. Latham, G. B. Mohanty, M. Pappagallo

Department of Physics, University of Warwick, Coventry CV4 7AL, United Kingdom

H. R. Band, X. Chen, B. Cheng, S. Dasu, M. Datta, K. T. Flood, J. J. Hollar, P. E. Kutter, B. Mellado,
A. Mihalyi, Y. Pan, M. Pierini, R. Prepost, S. L. Wu, Z. Yu

University of Wisconsin, Madison, Wisconsin 53706, USA

H. Neal

Yale University, New Haven, Connecticut 06511, USA

1 Introduction

Following the discovery of CP violation in B meson decays and the measurement of the angle β of the unitarity triangle [1] associated with the Cabibbo-Kobayashi-Maskawa (CKM) quark mixing matrix, focus has turned toward the measurements of the other angles α and γ . Following Ref. [2], several methods have been proposed to measure the relative weak phase between the $B^- \rightarrow D^0 K^-$ amplitude, proportional to the CKM matrix element V_{ub} (Fig. 1), and the $B^- \rightarrow \bar{D}^0 K^-$ amplitude, proportional to V_{cb} . This weak phase, which by definition ($\gamma = \arg(-V_{ub}^* V_{ud}/V_{cb}^* V_{cd})$) is γ , can be measured from the interference that occurs when the D^0 and the \bar{D}^0 decay to common final states.

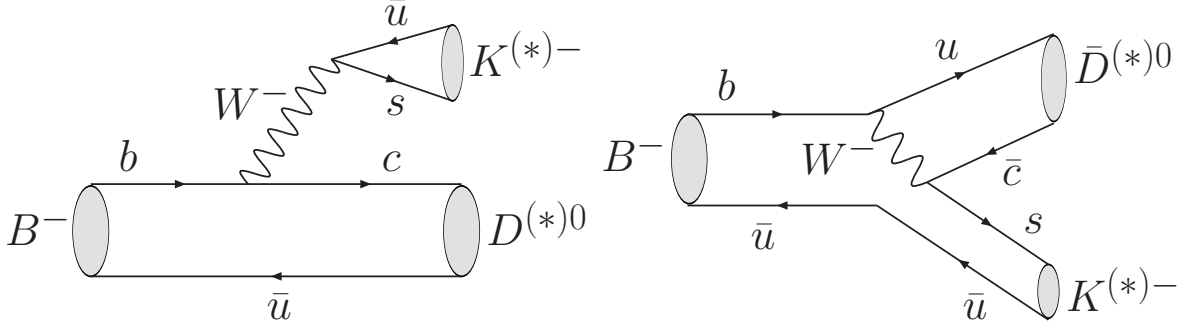


Figure 1: Feynman diagrams for the CKM-favored $B^- \rightarrow D^0 K^-$ and the CKM- and color-suppressed $B^- \rightarrow \bar{D}^0 K^-$ decays.

As an extension of the method proposed in Ref. [3], we search for $B^- \rightarrow [K^+ \pi^- \pi^0]_D K^-$ [4], where the CKM-favored $B^- \rightarrow D^0 K^-$ decay, followed by the doubly Cabibbo-suppressed $D^0 \rightarrow K^+ \pi^- \pi^0$ decay, interferes with the CKM-suppressed $B^- \rightarrow \bar{D}^0 K^-$ decay, followed by the Cabibbo-favored $\bar{D}^0 \rightarrow K^+ \pi^- \pi^0$ decay.

In order to reduce the systematic uncertainties, we measure ratios of branching fractions of the decay modes of interest in which the two kaons have opposite charge, referred to as “wrong sign” events, to the corresponding ones in favored decays, where the kaons have the same charge, referred to as “right sign” events. The two ratios we consider, to separate the sensitivity to the suppressed rate and the CP violation, are:

$$\begin{aligned}
 R_{ADS} &\equiv \frac{\Gamma([K^+ \pi^- \pi^0]_D K^-) + \Gamma([K^- \pi^+ \pi^0]_D K^+)}{\Gamma([K^+ \pi^- \pi^0]_D K^+) + \Gamma([K^- \pi^+ \pi^0]_D K^-)} \\
 &= r_B^2 + r_D^2 + 2r_B r_D C \cos \gamma \\
 A_{ADS} &\equiv \frac{\Gamma([K^+ \pi^- \pi^0]_D K^-) - \Gamma([K^- \pi^+ \pi^0]_D K^+)}{\Gamma([K^+ \pi^- \pi^0]_D K^-) + \Gamma([K^- \pi^+ \pi^0]_D K^+)} \\
 &= 2r_B r_D S \sin \gamma / R_{ADS}
 \end{aligned} \tag{1}$$

where D -mixing effects are neglected, $r_B \equiv \left| \frac{A(B^- \rightarrow \bar{D}^0 K^-)}{A(B^- \rightarrow D^0 K^-)} \right|$, $r_D^2 \equiv \frac{B(D^0 \rightarrow K^+ \pi^- \pi^0)}{B(\bar{D}^0 \rightarrow K^- \pi^+ \pi^0)}$, and the C and S parameters take into account the fact that the strong phases of the D decays are a function of the decay kinematics. Indicating with \vec{m} a point in the Dalitz plane $[m_{K\pi}^2, m_{K\pi^0}^2]$, with $[A_D(\vec{m}), \delta(\vec{m})]$ ($[\bar{A}_D(\vec{m}), \bar{\delta}(\vec{m})]$) the absolute value and the strong phase of the D (\bar{D}) decay amplitudes, and with

δ_B the strong phase difference between the two interfering B decays, we have

$$\begin{aligned}
C &= \frac{\int \mathcal{A}_D(\vec{m}) \overline{\mathcal{A}}_D(\vec{m}) \cos(\bar{\delta}(\vec{m}) - \delta(\vec{m}) + \delta_B(\vec{m})) d\vec{m}}{\sqrt{\int |\overline{\mathcal{A}}_D(\vec{m})|^2 d\vec{m} \cdot \int |\mathcal{A}_D(\vec{m})|^2 d\vec{m}}} \\
S &= \frac{\int \mathcal{A}_D(\vec{m}) \overline{\mathcal{A}}_D(\vec{m}) \sin(\bar{\delta}(\vec{m}) - \delta(\vec{m}) + \delta_B(\vec{m})) d\vec{m}}{\sqrt{\int |\overline{\mathcal{A}}_D(\vec{m})|^2 d\vec{m} \cdot \int |\mathcal{A}_D(\vec{m})|^2 d\vec{m}}}.
\end{aligned}
\tag{2}$$

Determining the angle γ from the measurements of R_{ADS} and A_{ADS} requires extracting the strong phases, for which the available statistics are insufficient. However, the value of r_B determines, in part, the level of interference between the diagrams of Fig. 1. In most techniques for measuring γ , high values of r_B lead to larger interference and better sensitivity to γ . Thus, r_B is a key quantity for the extraction of γ from other measurements in $B \rightarrow DK$ decays [5]. In this paper we therefore only measure R_{ADS} and we constrain r_B by exploiting the fact that in Eq. 1 $|C| < 1$.

Both the Belle and BABAR collaborations have published similar measurements but in a different decay chain ($B \rightarrow DK$ with $D \rightarrow K\pi$) [6]. Unlike those measurements, we can take advantage of the smaller value of r_D , which is $r_D^2 = (0.214 \pm 0.008 \pm 0.008)\%$ [7] in $D \rightarrow K\pi\pi^0$ decays as opposed to $r_D^2 = (0.362 \pm 0.020 \pm 0.027)\%$ [8] in $D \rightarrow K\pi$ decays. This implies that for a given error on R_{ADS} , the sensitivity to r_B is larger.

2 Event Reconstruction and Selection

The results presented in this paper are based on an 226×10^6 $\Upsilon(4S) \rightarrow B\bar{B}$ decays collected between 1999 and 2004 with the BABAR detector at the PEP-II B Factory at SLAC [9]. In addition, 15.8 fb^{-1} of off-resonance data, with center-of-mass (CM) energy 40 MeV below the $\Upsilon(4S)$ resonance, is used to study backgrounds from continuum events, $e^+e^- \rightarrow q\bar{q}$ ($q = u, d, s, \text{ or } c$). The BABAR detector is described elsewhere [10]. As far as this study is concerned, charged-particle tracking is provided by a five-layer silicon vertex tracker (SVT) and a 40-layer drift chamber (DCH). In addition to providing precise spatial hits for tracking, the SVT and DCH also measure the specific ionization (dE/dx), which is used for particle identification of low-momentum charged particles. At higher momenta ($p > 0.7 \text{ GeV}/c$) pions and kaons are identified by Cherenkov radiation detected in a ring-imaging device (DIRC). The typical separation between pions and kaons varies from 8σ at 2 GeV/ c to 2.5σ at 4 GeV/ c . The position and energy of neutral clusters (photons) are measured with an electromagnetic calorimeter (EMC) consisting of 6580 thallium-doped CsI crystals. These systems are mounted inside a 1.5-T solenoidal super-conducting magnet.

The event selection was developed from studies of $B\bar{B}$ and continuum events simulated with Monte Carlo techniques (MC), and of off-resonance data. A large on-resonance data sample of $B^- \rightarrow D^0\pi^-$, $D^0 \rightarrow K^-\pi^+\pi^0$ events was used to validate several aspects of the simulation and analysis procedure. We refer to this mode as $B \rightarrow D\pi$.

In the reconstruction, both kaon candidates are required to satisfy kaon identification criteria, which are based on specific ionization loss measured in the tracking devices and on Cherenkov angles in the DIRC and are typically 85% efficient, depending on momentum and polar angle. Misidentification rates are at the two percent level. The π^0 candidates are reconstructed as pairs of photon candidates in the EMC, each with energy larger than 70 MeV and lateral shower profile consistent with an electromagnetic deposit, with a total energy greater than 200 MeV, and with $118.25 < m_{\gamma\gamma} < 145.05 \text{ MeV}/c^2$. To account for the correlation between the tails in the distribution

of the $K\pi\pi^0$ invariant mass and the π^0 candidate mass, we require the difference between the two measured masses to be within $32.5 \text{ MeV}/c^2$ of the expected value of $1729.5 \text{ MeV}/c^2$ [11]. The remaining background from other $B^\pm \rightarrow [h_1 h_2 \pi^0]_D h_3^\pm$ [4] modes is reduced by removing events where any $h_1 h_2 \pi^0$ candidate, with any particle-type assignment except for the signal hypothesis for the $h_1 h_2$ pair, is consistent with a D^0 meson decay.

After these requirements, the background is mostly due to $e^+e^- \rightarrow c\bar{c}$ events, with $\bar{c} \rightarrow \bar{D}^0 \rightarrow K^+\pi^-\pi^0$ and $c \rightarrow D \rightarrow K^-$. In order to discriminate against them we use a neural network (NN) with six quantities that distinguish continuum and $B\bar{B}$ events: (i) $L_0 = \sum_i p_i$ and (ii) $L_2 = \sum_i p_i \cos^2 \theta_i$, both calculated in the CM frame. Here, p_i is the momentum and θ_i is the angle with respect to the thrust axis of the B candidate of tracks and clusters not used to reconstruct the B . (iii) The angle in the CM frame between the thrust axes of the B and of the detected remainder of the event. (iv) The polar angle of the B candidate in the CM frame. (v) The distance of closest approach between the bachelor track and the trajectory of the D meson. This is consistent with zero for signal events, but can be larger in $c\bar{c}$ events. (vi) the distance along the beams between the reconstructed vertex of the B candidate and the vertex of the other tracks in the event. This is consistent with zero for continuum events, but is sensitive to the B lifetime for the signal events.

The NN is trained with simulated continuum and signal events. We find agreement between the distributions of all six variables in simulation and in control samples of off-resonance data and of $B \rightarrow D\pi$ events. We apply a loose pre-selection on the NN ($0.4 < NN < 1.0$) with a 90% efficiency on signal and a 68% rejection power over continuum, but then use the NN itself in the likelihood fit to fully exploit its discriminant power.

A B candidate is characterized by the energy-substituted mass $m_{\text{ES}} \equiv \sqrt{(\frac{s}{2} + \vec{p}_0 \cdot \vec{p}_B)^2 / E_0^2 - p_B^2}$ and energy difference $\Delta E \equiv E_B^* - \frac{1}{2}\sqrt{s}$, where E and p are energy and momentum, the asterisk denotes the CM frame, the subscripts 0 and B refer to the initial e^+e^- state and B candidate, respectively, and s is the square of the CM energy. For signal events m_{ES} is centered around the B mass with a resolution of about $2.5 \text{ MeV}/c^2$, and ΔE is centered at zero with an RMS of 0.017 GeV .

Considering both the right sign and the wrong sign sample, 28621 events survive the selection described above and the loose requirements $|\Delta E| < 100 \text{ MeV}$ and $m_{\text{ES}} > 5.2 \text{ GeV}/c^2$. The dominant background still comes from continuum events, but we also need to take into account background from $\Upsilon(4S) \rightarrow B\bar{B}$ (“ $B\bar{B}$ ”) events. We consider separately the $B \rightarrow D\pi$ background since it differs from the signal only in the ΔE distribution. This decay mode has a very low value of r_B ($\sim r_B(D^0 K)\lambda^2$, where $\lambda \sim 0.22$ is the sine of the Cabibbo angle), and therefore in the likelihood fit we will consider it as a background only for the right sign sample.

3 Likelihood Fit and Results

The signal and background yields are extracted by maximizing the extended likelihood $\mathcal{L} = e^{-N'} \prod_{i=1}^{N'} \mathcal{L}_i(x_i) / N'!$. Here $N' = N_{DK} + N_{\text{cont}} + N_{BB} + N_{D\pi}$ is the sum of the yields of the signal and the three background contributions, $\vec{x} = \{NN, \Delta E, m_{\text{ES}}\}$, and the likelihood of the individual events (\mathcal{L}_i) is defined as

$$\begin{aligned} \mathcal{L}(\vec{x}) = & \frac{N_{DK}}{1 + R_{ADS}} f_{DK}^{RS}(\vec{x}) + \frac{N_{\text{cont}}^{RS}}{1 + R_{\text{cont}}} f_{\text{cont}}^{RS}(\vec{x}) \\ & + \frac{N_{BB}}{1 + R_{BB}} f_{BB}^{RS}(\vec{x}) + N_{D\pi} f_{D\pi}(\vec{x}) \end{aligned} \quad (3)$$

for right sign events and

$$\begin{aligned} \mathcal{L}(\vec{x}) = & \frac{N_{DK}R_{ADS}}{1 + R_{ADS}} f_{DK}^{WS}(\vec{x}) + \frac{N_{cont}R_{cont}}{1 + R_{cont}} f_{cont}^{WS}(\vec{x}) \\ & + \frac{N_{BB}R_{BB}}{1 + R_{BB}} f_{BB}^{WS}(\vec{x}) \end{aligned}$$

for wrong sign events.

We have defined R parameters for the backgrounds with the same definition as in Eq. 1. The individual probability density functions (f) are derived from the MC and the three variables are considered uncorrelated in all cases, apart from m_{ES} and ΔE for the $D\pi$ background, since the correlations are not negligible. For the latter we have therefore utilized a two dimensional non-parametric distribution [12]. The NN distributions are all modeled with a histogram with eight bins between 0.4 and 1. The m_{ES} distributions are modeled with a Gaussian in the case of the signal, a threshold function [13] in the case of the continuum background, and the sum of a threshold function and a Gaussian function with an exponential tail in the case of the $B\bar{B}$ background. Finally, the ΔE distributions are parametrized with the sum of two Gaussians in the case of the signal, an exponential in the case of the continuum background, and a double exponential in the case of the $B\bar{B}$ background.

We perform the fit by floating the four total yields (N_{DK} , N_{cont} , N_{BB} , and $N_{D\pi}$), the three R variables and the shape parameters of the threshold function used to parametrize m_{ES} for the same and opposite sign continuum background. Figure 2 shows the distributions of the three variables in the selected sample (separately for same sign and opposite sign events), with the likelihood projections overlaid. The fit yields $R_{ADS} = 0.012^{+0.012}_{-0.010}$, $N_{DK} = (14.7 \pm 0.6) \times 10^2$, $N_{cont} = (239.3 \pm 2.1) \times 10^2$, $N_{BB} = (25.5 \pm 1.6) \times 10^2$, $N_{D\pi} = (6.7 \pm 0.4) \times 10^2$, $R_{cont} = 3.05 \pm 0.07$, $R_{BB} = 0.42 \pm 0.07$.

Equation 3 assumes that the efficiencies are the same between the right and the wrong sign signal samples, regardless of the different Dalitz structure. This has been tested on MC and proved to be true within a statistical error of 4%. We then consider this as a systematic error on R_{ADS} . We also repeated the fit by varying the probability density function parameters obtained with MC within their statistical errors and by estimating $f_{cont}^{RS/WS}$ on off-resonance data and $f_{DK}^{RS/WS}$ on exclusively reconstructed $D\pi$ events. To account for the observed variations, we assign a 0.008 systematic error on R_{ADS} . The uncertainty due to B decays with distributions similar to the signal, in particular $B \rightarrow D^{(*)}\pi$, D^*K , $D^{(*)}K^*$, and $KK\pi\pi^0$, is estimated by varying their branching fractions within their known errors and found to be 0.00006 on R_{ADS} , and therefore negligible. The absence of further modes which might fake signal has been checked comparing data and MC samples in the sidebands of the ΔE and $m_{D^0} - m_{\pi^0}$ distributions.

Following a Bayesian approach, we extract r_B by defining the a posteriori probability

$$\mathcal{L}(r_B) = \frac{\int p(r_B, r_D, \xi) \mathcal{L}(R_{ADS}(r_B, r_D, \xi)) dr_D d\xi}{\int p(r_{D^0K^+}, r_D, \xi) \mathcal{L}(R_{ADS}(r_B, r_D, \xi)) dr_D d\xi dr_B}, \quad (4)$$

where $\xi = C \cos \gamma$, $R_{ADS}(r_B, r_D, \xi)$ is given in Eq. 1, and $p(r_B, r_D, \xi)$ is the a priori probability for these three quantities. They are considered uncorrelated, with ξ and r_B distributed flat in the range $[-1, 1]$ and $[0, 1]$ respectively. The a priori probability for r_D is a Gaussian consistent with $r_D^2 = (0.214 \pm 0.008 \pm 0.008)\%$ [7]. The likelihood $\mathcal{L}(R_{ADS})$ is obtained by convolving the likelihood returned by the fit with a Gaussian of width 0.0076, equivalent to the systematic uncertainty.

Figure 3 shows $\mathcal{L}(R_{ADS})$ and $\mathcal{L}(r_B)$. We set a 95% confidence level (C.L.) limit, by integrating the likelihood starting from $R_{ADS} = 0$ ($r_B = 0$), thus excluding unphysical values, and we define

the 68% C.L. region, for each variable $r = R_{ADS}$ or r_B , as the interval where $\mathcal{L}(r) > \mathcal{L}_{min}$ and $68\% = \int_{\mathcal{L}(r) > \mathcal{L}_{min}} \mathcal{L}(r) dr$.

4 Conclusions

In summary, we measure the ratio of the rate for the $B^\pm \rightarrow [K^\mp \pi^\pm \pi^0]_D K^\pm$ decay to the favored decay $B^\pm \rightarrow [K^\pm \pi^\mp \pi^0]_D K^\pm$ to be $R_{ADS} = 0.012_{-0.010}^{+0.012}(\text{stat})_{-0.007}^{+0.010}(\text{sys})$. This result is consistent in central value and similar in sensitivity with our completely independent previously published result [6]. The measurement is not significant and therefore we set a 95% C.L. limit $R_{ADS} < 0.039$. We use this information to infer the ratio of the magnitudes of the $B^- \rightarrow \bar{D}^0 K^-$ and $B^- \rightarrow D^0 K^-$ amplitudes to be $r_B = 0.091 \pm 0.059$ and consequently set a limit $r_B < 0.185$ at 95% C.L.

We are grateful for the extraordinary contributions of our PEP-II colleagues in achieving the excellent luminosity and machine conditions that have made this work possible. The success of this project also relies critically on the expertise and dedication of the computing organizations that support *BABAR*. The collaborating institutions wish to thank SLAC for its support and the kind hospitality extended to them. This work is supported by the US Department of Energy and National Science Foundation, the Natural Sciences and Engineering Research Council (Canada), Institute of High Energy Physics (China), the Commissariat à l’Energie Atomique and Institut National de Physique Nucléaire et de Physique des Particules (France), the Bundesministerium für Bildung und Forschung and Deutsche Forschungsgemeinschaft (Germany), the Istituto Nazionale di Fisica Nucleare (Italy), the Foundation for Fundamental Research on Matter (The Netherlands), the Research Council of Norway, the Ministry of Science and Technology of the Russian Federation, Ministerio de Educación y Ciencia (Spain), and the Particle Physics and Astronomy Research Council (United Kingdom). Individuals have received support from the Marie-Curie IEF program (European Union) and the A. P. Sloan Foundation.

References

- [1] BaBar Collaboration, B. Aubert *et al.*, Phys. Rev. Lett. **89**, 201802 (2002); Belle Collaboration, K. Abe *et al.*, Phys. Rev. **D66**, 071102 (2002).
- [2] M. Gronau and D. Wyler, Phys. Lett. **B265**, 172 (1991); M. Gronau and D. London, Phys. Lett. **B253**, 483 (1991).
- [3] D. Atwood, I. Dunietz, and A. Soni, Phys. Rev. Lett. **78**, 3257 (1997); Phys. Rev. **D63**, 036005 (2001).
- [4] Charge conjugation is implied throughout the paper. Also, we use the notation $B^- \rightarrow [h_1^+ h_2^- \pi^0]_D h_3^-$ (with $h_i = \pi$ or K) for the decay chains $B^- \rightarrow \tilde{D}^0 h_3^-$, where \tilde{D}^0 is either a D^0 or a \bar{D}^0 and $\tilde{D}^0 \rightarrow h_1^+ h_2^-$. We also refer to h_3 as the bachelor π or K .
- [5] BaBar Collaboration, B. Aubert *et al.*, Phys. Rev. Lett. **95**, 121802 (2005).
- [6] BaBar Collaboration, B. Aubert *et al.*, Phys. Rev. D **72**, 032004 (2005); Belle Collaboration, M. Saigo *et al.*, Phys. Rev. Lett. **94** 091601 (2005).
- [7] "Search for $D^0 - \bar{D}^0$ mixing and a measurement of the doubly Cabibbo-suppressed rate in the decay $D^0 \rightarrow K^+ \pi^- \pi^0$, BaBar Collaboration, in preparation.

- [8] BaBar Collaboration, B. Aubert *et al.*, Phys. Rev. Lett. **91**, 171801 (2003).
- [9] PEP-II Conceptual Design Report, SLAC-0418 (1993).
- [10] BaBar Collaboration, B. Aubert *et al.*, Nucl. Instrum. and Methods Phys. Res., Sec. **A 479**, 1 (2002).
- [11] Particle Data Group, S. Eidelman *et al.*, Phys. Lett. B **592**, 1 (2004).
- [12] K. Cranmer, Comput. Phys. Commun. **136**, 198 (2001).
- [13] ARGUS Collaboration, H. Albrecht *et al.*, Z. Phys. C **48**, 543 (1990).

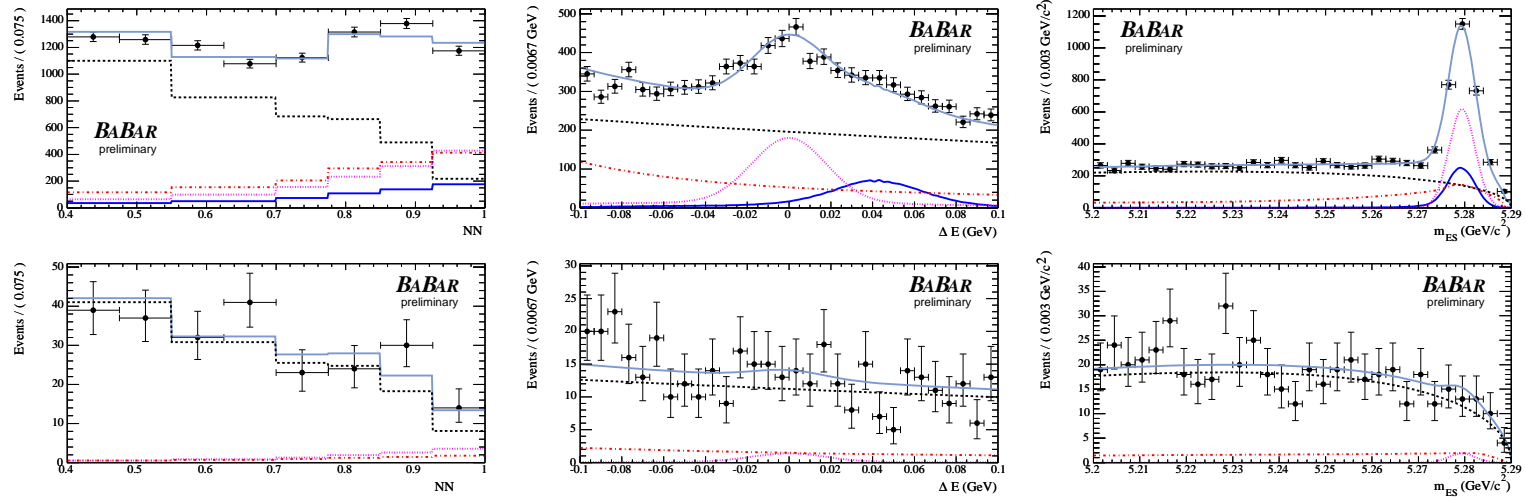


Figure 2: Likelihood fit projection of the NN , ΔE , and m_{ES} distributions separately for the same (top) and opposite (bottom) sign sample. To visually enhance the signal, the distributions for the latter sample are shown after cuts, with a 67% signal efficiency, on the ratios between the signal and the signal plus background likelihood of all the variables other than the one shown. The points with error bars represent the data while the dashed, dash-dotted, and solid lines represent the contribution from continuum, $B\bar{B}$, and $D\pi$ background, respectively. The dotted line represents the signal contribution, visible only in the same sign sample.

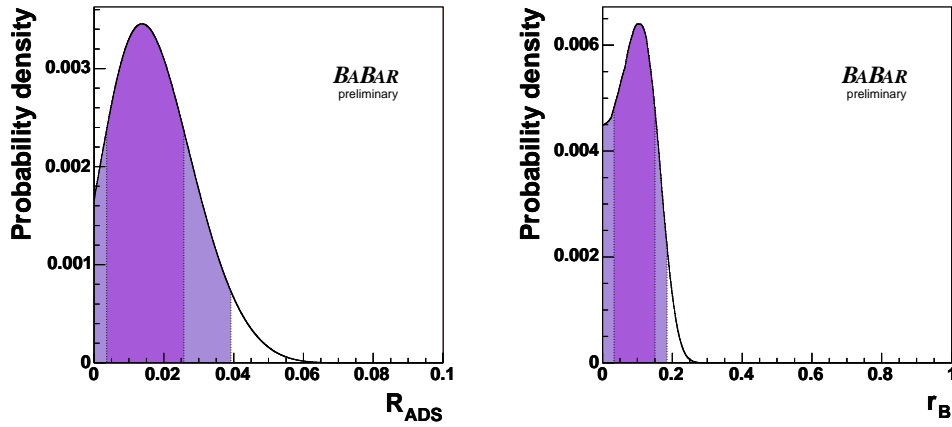


Figure 3: Likelihood as a function of R_{ADS} (left) and of r_B (right). While the left plot shows the actual experimental result of the measurements, the right plot is obtained in a bayesian approach assuming flat prior distributions for r_B , C and γ . The 68% and 95% region are shown in dark and light shading respectively.